Droplet-on-demand Inkjet-filled Through-silicon Vias (TSVs) as a Pathway to Cost-efficient Chip Stacking

Jacob Sadie, Niels Quack, Ming C. Wu, and Vivek Subramanian
Department of Electrical Engineering and Computer Sciences
University of California, Berkeley
Berkeley, CA 94720 U.S.A
Ph: 510-643-4535; Fax: 512-642-2739
Email: jake.sadie@berkeley.edu

Abstract
Using metal nanoparticle-based inks and droplet-on-demand inkjet printing, we have demonstrated the ability to fully fill, bump, and bond through-silicon vias (TSVs). Standard thermo-compression flip-chip bonding is used to provide both robust mechanical as well as electrical contact while processing below conventional back-end-of-line (BEOL) thermal budgets. This novel process enables both the filling and bumping of TSVs in a single process step, making this process unique among conventional TSV process flows and providing a cost-effective alternative for three-dimensional integration and chip stacking at both the die-level and wafer-scale.

Key words
Inkjet printing, metal nanoparticle, TSV, droplet-on-demand, three-dimensional integration.

I. Introduction

Though still a nascent area of research and development, TSV technologies have rapidly progressed due to their highly anticipated ability to enable chip stacking, heterogeneous integration schemes, and the perpetuation of Moore's Law [1]. Common approaches for TSV filling currently involve copper electroplating [2], tungsten CVD [3], and isolated highly-doped silicon columns [4]. Each of these techniques is tuned for wafer-scale process flows, requires multiple processing steps, and requires large volumes of material to fabricate the final feature. In addition, the TSV features require a separate solder bump process prior to bonding. Therefore, in order to create a more pervasive TSV process technology, significant cost scaling to the current processes is necessary. A via filling strategy that 1) scales well for medium- to high-density TSV layouts, 2) requires minimal materials, 3) maintains thermal budget restrictions established for BEOL processing, and 4) enables both die-scale and wafer-scale fabrication compatibility will be a particularly impactful achievement.

Previously, we have demonstrated the use of metal nanoparticle inks for lead-free solder bump replacement in advanced packaging applications [5]. Metal nanoparticles are particularly interesting because they provide high conductivity interconnects at relatively low sinter temperatures as well as excellent mechanical and thermal reliability. In this work, we take advantage of the same principles learned from freestanding pillar fabrication and apply them to filling processes in order to both fill and bump pre-fabricated deep reactive ion etched (DRIE) TSVs in a single process step.

The critical process step for the realization of high-conductivity interconnects comprised of nanoparticle-based inks is sintering. During sintering, the material is heated and the bonds between the carbon-based organic encapsulant and metal nanoparticle core break, allowing for the ultimate coalescence of the nanoparticle cores into an electrically continuous feature. A proposed sintering mechanism for freestanding pillars was discussed in our previous work [5], however the more confined geometry of a TSV is expected to lead to non-trivial differences in sintering behavior. Namely, the redistribution of diffusing encapsulant material may lead to increased TSV resistance compared to pillar resistance for a given geometry and sintering condition. Furthermore, the sintering process is often described by a two-step process where the first step involves the removal of the encapsulant and permits particle (and encapsulant) diffusion and the second step involves particle growth into a denser film [6]. Compared to conventional reflow processes, nanoparticle sintering in three-dimensional films may take advantage of this particle (and encapsulant) diffusion process in order to mimic the lead-tin solder reflow processes necessary for die-leveling and bonding.

To our knowledge, metal nanoparticles have thus far only been used to partially fill TSVs [7]. We have recently reported on using nanoparticle inks to completely fill TSVs [8]. This work represents the first demonstration of a complete BEOL process for filling, bumping, and bonding (*including reflow*) TSVs using nanoparticle-based inks.

II. Experimental Setup

A. TSV Preparation

All TSVs presented in this work were fabricated using a standard DRIE Bosch process. 100 µm deep TSV trenches were etched into either 6” silicon or 6” SOI substrates (100 µm device layer, 2 µm buried oxide (BOX), and 500 µm handle) in both square and circular features. Critical feature dimensions (square side length and circle diameter) ranged from 10-100 µm. Features were etched in square arrays with pitches equal to 1.5, 2, and 2.5 times the critical dimension. For the purposes of electrical testing, an approximately 130 nm layer of low-temperature oxide (LTO) was deposited to isolate the TSVs from the highly-doped device layer. Finally, wafers were diced into individual die using a Disco DAD3240 dicing saw for subsequent printing and bonding.

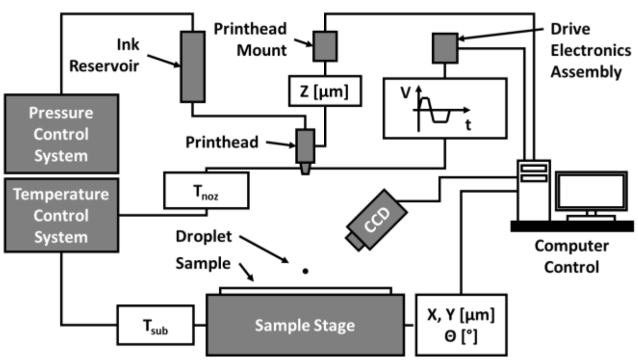

Fig. 1. Schematic for custom inkjet printer.

B. Inkjet Printing

Inkjet printing was performed using a custom-built droplet-on-demand inkjet printer (see Fig. 1). All TSVs were filled and bumped using Harima NPG-J gold nanoparticle ink (nanoparticle diameter ~4-6 nm) and a 60 µm MicroFab piezoelectrically-driven inkjet nozzle. Similar to freestanding pillar fabrication, the two main process parameters for TSV filling and bumping were substrate temperature as well as the time between subsequent drops on a given feature. In order to fabricate bumps on top of the TSVs, additional drops were placed immediately following TSV filling much in the same way pillars were formed on flat surfaces in our prior work (see Fig. 2). For these TSVs, 140 °C substrate temperatures and 7 second drop delays proved suitable for both filling and bumping processes.

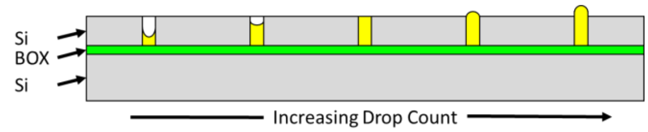

Fig. 2. TSV filling and bumping on an SOI die.

C. Bonding

Thermo-compression bonding was performed using a Finetech Fineplacer Lambda flip-chip bonder. The force used for bonding was 1 N and the bonding temperature was 250 °C in accordance with the prescribed sinter temperature for Harima NPG-J ink. Die bonded in this work were all bonded for ten minutes. In this work, direct die-to-die and die-to-wafer bonds are demonstrated. Fig. 3 shows typical boding process schemes.

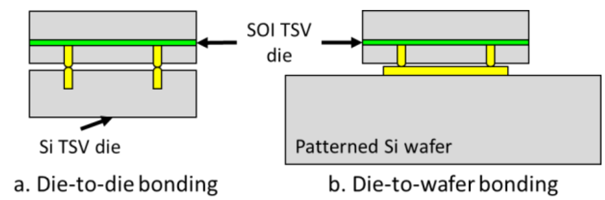

Fig. 3. Filled and bumped SOI TSV die bonded to a) filled and bumped Si TSV die and b) patterned Si wafer.

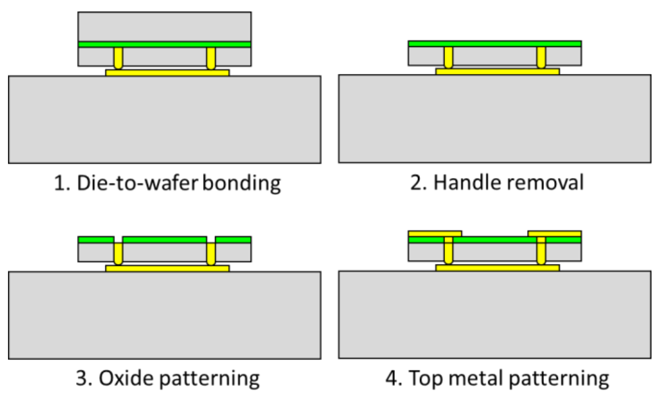

Fig. 4. Backside processing flow for electrical testing.

D. Mechanical and Electrical Testing

Mechanical and electrical testing of die bonded to carrier substrates were performed using a Nordson Dage 4000 bond tester and four-point probe setup, respectively. Mechanical shear tests were performed at a shear rate of 300 µm/s. To fabricate die for electrical testing, the handle of the SOI was removed using an isotropic SF_6 dry plasma etch. The BOX was patterned and etched with buffered oxide etch (BOE). The BOX was patterned again and a layer of metal was evaporated on top of the structure to create a daisy chain structure via liftoff. Refer to Fig. 4 for the complete process flow.

E. TSV Imaging

SEM images presented were taken using a Zeiss LEO scanning electron microscope. Confocal microscope images presented were taken using an Olympus LEXT OLS3000 3D laser confocal microscope. A Keyence VHX-600 digital microscope was used to image bonded die interfaces.

III. Results and Discussion

A. Filling and Bumping

Ideal TSV filling should provide a dense, void-free plug. Because metal nanoparticle inks contain both organic-encapsulated nanoparticles as well as a carrier solvent for dispensing the material, it is critical to remove as much of this solvent as possible *during printing* to obtain dense films. Residual solvent trapped inside the TSV may lead to pores or cracking/compaction during the sintering process and introduce voids in the TSVs. Therefore, analogous to pillar fabrication, adjusting the substrate temperature as well as the delay time between drops allows us to successfully remove solvent material during the printing process. However, the TSV structure is more confined than the freestanding pillar case, requiring higher substrate temperatures and longer wait times to ensure the complete evaporation of the carrier solvent.

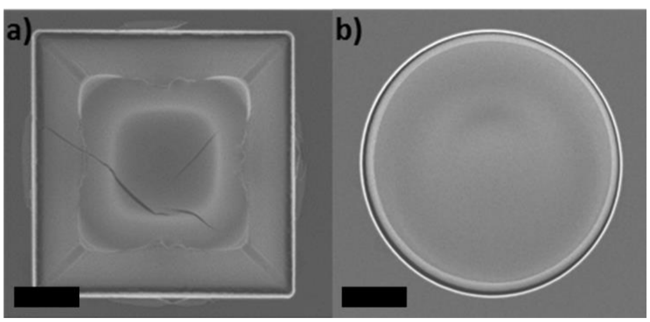

Fig. 5. 80 µm critical dimension a) square and b) circular TSVs. Scale bar is 20 µm.

TSVs are filled in a dropwise manner by directly depositing ink into the etched trenches in the substrate. Because a 60 µm nozzle was used for this work, the lower bound for TSV critical dimension achieved was 60 µm, though decreasing the nozzle dimension should readily enable filling smaller critical dimension TSVs.

Fig. 5 presents a top-down SEM view of a square and circular via with critical dimension of 80 µm. The number of drops in each TSV is identical, the drop count was tuned to fully fill the circular via. If tuned properly, the filling process will result in a flat surface near the top of the trench. This surface will enable the bumping of filled TSVs using the same process parameters. Fig. 6 is a demonstration of filled and bumped TSVs in a square array. The inset of Fig. 6 is an example of bumps actually beginning to form beneath the top surface of the trench. The vertical position for the onset of pillar growth can be tuned by adjusting the printing parameters.

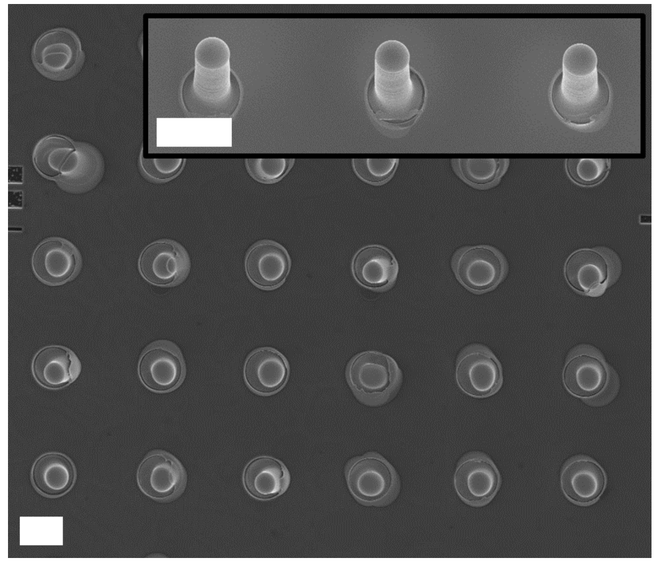

Fig. 6. Top-down SEM view of printed TSV array. Inset: Zoomed view of pillars extending out of circular TSVs (not the same die). Scale bars are 100 µm.

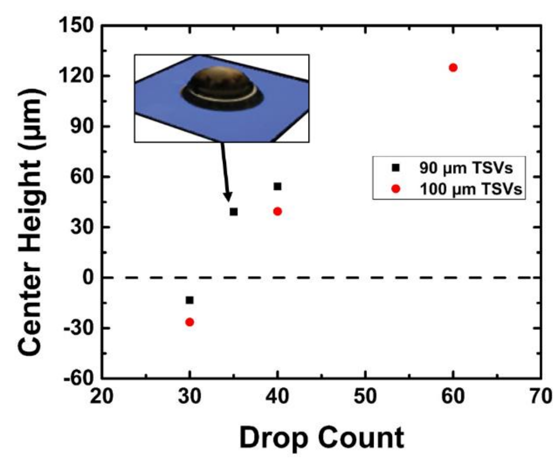

Fig. 7. TSV filling as a function of drop count. Inset: Representative confocal microscope image for bumped TSV.

Confocal laser microscopy was used to rapidly determine the fill level of as-printed TSV features. The graph in Fig. 7 represents the fill level of the printed TSVs as a function of drop count for two different circular TSV dimensions. The measurements are referenced to the top surface of the trench, therefore, negative values indicate incompletely filled TSVs and positive values indicate bumped TSVs. The image in the inset of Fig. 7 is an example of the output from the confocal microscope for a bumped TSV feature.

In order to confirm compact filling, printed TSVs were sintered and diced into cross-sections. The SEM images in Fig. 8 indicate compact post-sinter filling for non-bonded TSVs. In these TSVs, the drop counts were 50, 70, and 90 total drops. In the 50 drop case, no bump has formed. In the 70 and 90 drop cases, however, a bump has formed and extended beyond the surface of the trench, but the dicing process resulted in damaging the top portion of these bumps. It may be noted that the drop count differs for features in Fig. 7 and Fig. 8, which is explained by performing the experiments with different printing pulse waveform parameters that led to different drop volumes. The cross section views in Fig. 8 further reveal small gaps between the filling material and the sidewall for some of the TSV. Possible reasons for the gap formation include detachment due to the shear force of the dicing blade during dicing, compaction during sintering, and/or poor adhesion between the ink and sidewall.

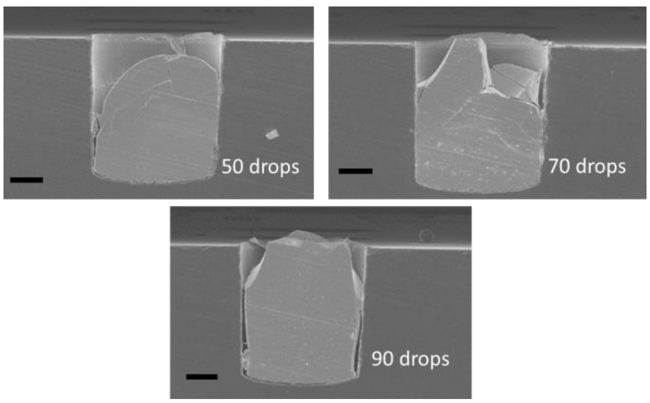

Fig. 8. Cross-sectional SEM of TSV filling as a function of drop count. All scale bars are 20 µm.

B. Bonding and Reflow

Bonding trials were performed on die-to-die and die-to-wafer cases. In die-to-die bonds, two 4 mm x 4 mm die were individually filled and bumped, but not sintered, and then bonded together. In die-to-wafer bonds, a single filled and bumped die was bonded to a silicon substrate with pre-patterned metal bond pads. The bonding temperature reached 250 °C in order to perform an in-situ sinter during the bonding process.

A critical property of conventional solder bumps is the ability to reflow, permitting bonded die to be leveled assuming non-uniform solder bumps across the die surface. Because non-uniformity in inkjet-printed nanoparticle bumps is also a reasonable expectation, reflow will be critical for enabling this technology as a drop-in replacement for solder bump deposition.

The cross-section SEM image in Fig. 9 is an example of die-to-die bonding. Similar to the non-bonded TSV cross-sections, these bonded die exhibit excellent material compaction. In addition, the TSVs are almost completely filled, despite initially being partially full with bumps extending beyond the trench surface. The voids at the sidewalls are still present, though these voids may be introduced due to the same reasons explained for die shown in Fig. 8.

These completely filled TSV bonds indicate that some amount of reflow must have occurred and side-view video capture during bonding was used to confirm reflow. Before reaching the peak bond temperature, a large gap is present between the two filled and bumped die (that are aligned bump-to-bump). Once the temperature reaches approximately 200 °C, the top die very rapidly collapses onto the bottom die and the gap disappears. This movement could only be facilitated by the redistribution of bumped material, and is analogous to conventional bump reflow. Comparing the filled TSVs in Fig. 10 shows two screen shots before and after the bonding process.

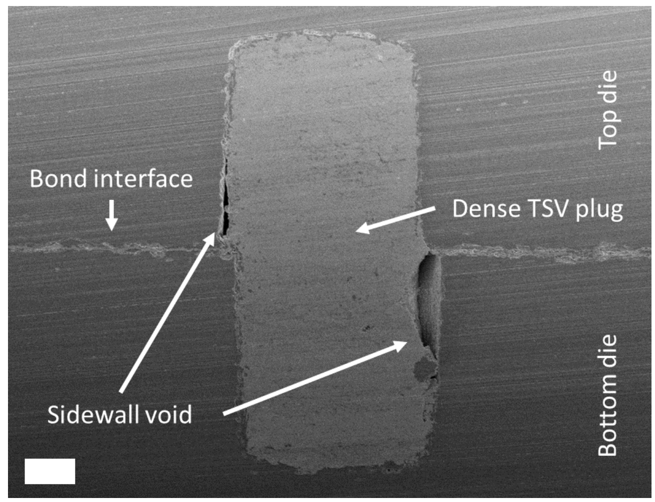

Fig. 9. Cross-sectional SEM of die-to-die bonding of 80 µm critical dimension circular TSVs showing dense filling. Scale bar is 20 µm.

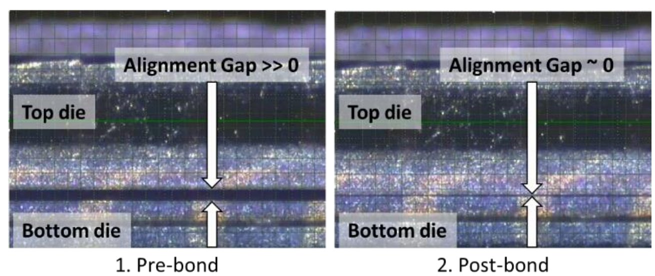

Fig. 10. Side-view screenshots taken before and after flip-chip bonding showing the disappearance of the alignment gap and indicating reflow.

C. Mechanical Characterization

To characterize the strength of nanoparticle-based solder bumps, 4 mm x 4 mm die were filled and bumped in a full 12 x 12 array, bonded to an array of gold bond pads on a 16 mm x 16 mm silicon substrate, and sheared using a Dage 4000 bond tester. Fig. 11 shows a representative die shear experiment where the maximum shear strength of the die reached 1.9 kg_F, or approximately 13.2 g_F per bond.

A second set of filled, bumped, bonded, and sheared die were prepared to judge the extent of reflow occurring during bonding. All die were prepared under identical printing and bonding conditions and only the drop count was varied. Excessive reflow, facilitated by unnecessarily large bumps (i.e. high drop counts), may lead to short circuits and decrease the minimum pitch attainable for bonding. Post rupture analysis confirmed failure at the bond interface, as shown in Fig. 12. The post rupture top views of three experiments show, that a higher drop count leads to a larger extent of reflow beyond the pads. This further confirms reflow but also indicates the need for a carefully tuned process in order to control the volume of the bump and avoid detrimental short-circuiting.

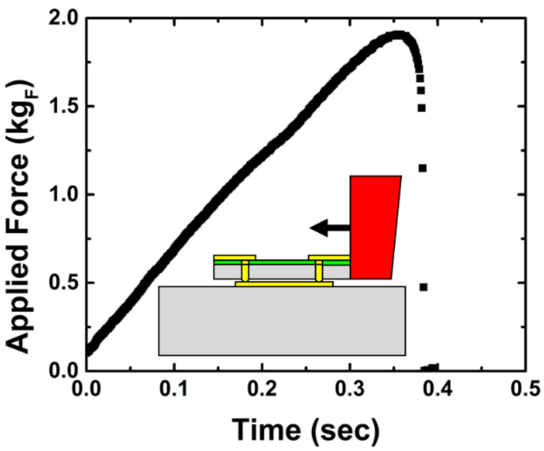

Fig. 11. Sample die shear experimental data showing shear strength of 1.9 kg_F. Inset: Schematic shear test setup.

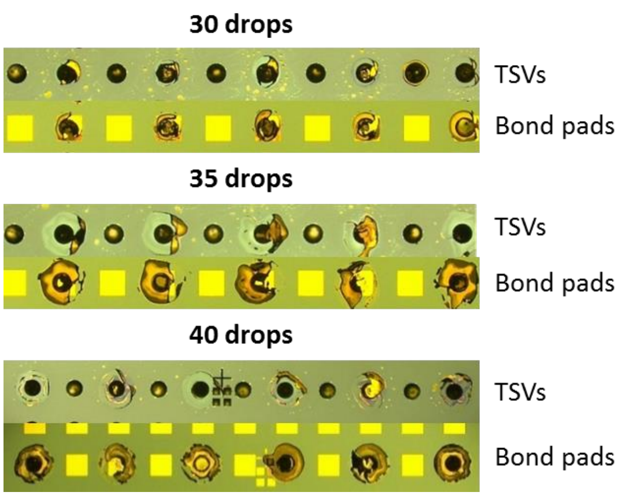

Fig. 12. Digital micrographs of shear interfaces for 90 µm critical dimension circular TSVs and bond pads as a function of drop count In each of the three samples, the top image is a top view of the TSVs and the bottom image is a top view of the bond pads.

D. Electrical Characterization

The process flow outlined in Fig. 4 enabled both top and bottom contact in a daisy-chain structure for the purposes of extracting the electrical properties of inkjet-filled TSVs. Fig. 13 shows a fully processed die prepared for electrical testing. The highest conductivity TSV measurement achieved for initial experiments provided a total extracted resistance of 800 mΩ for a single TSV with diameter of 100µm. After subtracting the line resistance associated with bottom die 50 nm gold interconnect and assuming the two TSVs under test each have equivalent resistance values, and approximating the test structure as a 100 µm tall, 50 µm radius cylinder, the extracted resistance per TSV is measured to be approximately 35 mΩ.

Table 1 summarizes how these TSVs compare to the highest conductivity freestanding pillars obtained in our previous work and the bulk conductivity of gold. As the table shows, the TSV conductivity is an order of magnitude below pillars which are themselves an order of magnitude lower than bulk gold. A deeper parametric study of bonding conditions will most likely lead to further improvements in the electrical performance of these structures though sub-ohm initial performance is very promising.

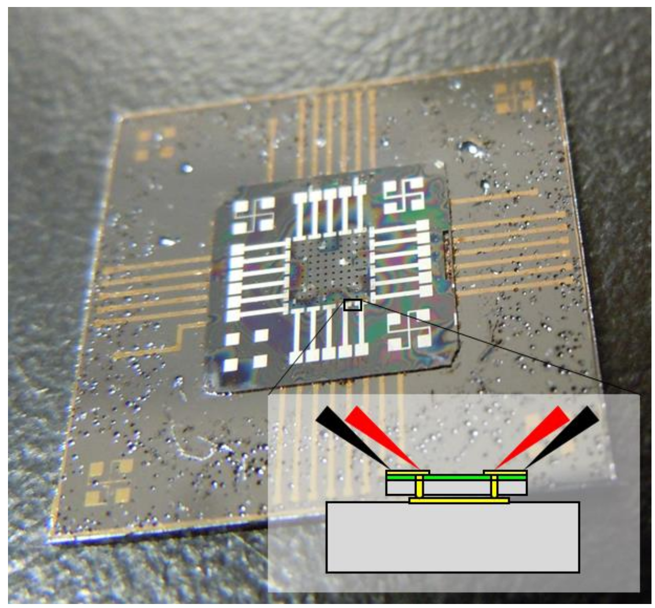

Fig. 13. Fully-processed electrical test die. Inset: Four-point probe measurement schematic.

Table 1. Comparison of highest conductivity features achieved to date for freestanding pillars and TSVs.

	Extracted Resistance (Ω)	Conductivity (S/cm)
TSV	3.5×10^{-2}	3.34×10^{3}
Pillar	1.2×10^{-2}	7.58×10^{4}
Bulk Gold	N/A	4.54×10^{5}

IV. Conclusion

This work presents the first single, inkjet-based, drop-in replacement process for both TSV filling and bumping while maintaining BEOL standard thermal budget constraints. Taking advantage of low sinter temperature, high conductivity metal nanoparticle inks, we are able to fill, bump, and bond DRIE-prepared TSVs and confirm dense TSV filling, evidence of reflow in inherently thick-film nanoparticle sintering, and robust electrical and mechanical interconnection between bonded die.

Acknowledgment

Portions of this work were supported by Ultratech, Inc. Dr. Quack is supported by the Defense Advanced Research Projects Agency (DARPA) E-PHI program under Grant No. HR0011-11-2-0021. The TSV trench and bonding substrates and imaging characterization tools were fabricated and supported by the Marvell Nanofabrication Laboratory at the University of California, Berkeley.

References

[1] N. Quack et al., “Development of an FMCW LADAR Source Chip using MEMS-Electronic-Photonic Heterogeneous Integration,” GOMACTech Conference, 13-4, Las Vegas, NV, USA, March 12-14, 2013.

[2] U. Kang et al., “8 Gb 3-D DDR3 DRAM Using Through-Silicon-Via Technology,” IEEE Journal of Solid-State Circuits, Vol. 45, No. 1, 2010, pp. 111-119.

[3] J. Burns et al., “A Wafer-scale 3-D Circuit Integration Technology,” IEEE Transactions on Electron Devices, Vol. 53, No. 10, 2006, pp. 2507-2516.

[4] M. Rimskog and T. Bauer, “High density through silicon vias (TSV),” 2008 Symposium on Design, Test, Integration and Packaging of MEMS/MOEMS, Nice, France, 9-11 April 2008.

[5] J. Sadie, S. Volkman, and V. Subramanian, “Demonstration of Inkjet-printed Nanoparticle-based Inks for Solder Bump Replacement,” in *Proc. of 2012 45th International Symposium on Microelectronics*, San Diego, CA, USA, Sept. 2012, pp. 419-424.

[6] L. Huang, “Sintering Metal Nanoparticle Films,” Ph.D. dissertation, Dept. of Mat. Sci. and Eng., Binghamton Univ., Vestal, New York, 2012.

[7] A. Rathjen, Y. Bergmann, and K. Kruger, “Feasibility Study: Inkjet Filling of Through Silicon Vias (TSV),” in *NIP28: International Conference on Digital Printing Technologies and Digital Fabrication 2011*, Quebec, Canada, Sept. 2012, pp. 454-460.

[8] N. Quack, J. Sadie, V. Subramanian, and M. C. Wu, “Through Silicon Vias and Thermocompression Bonding Using Inkjet-Printed Gold Nanoparticles For Heterogeneous MEMS Integration,” in *Proc. of 17th International Conference on Solid-State Sensors, Actuators, and Microsystems*, Barcelona, Spain, June 2013, pp. 834-837.